Available online at www.sciencedirect.com
SCIENCE DIRECT®
Journal of Sound and Vibration 282 (2005) 265–276
JOURNAL OF SOUND AND VIBRATION
www.elsevier.com/locate/jsvi

Two-dimensional vibrations of air-filled geomembrane tubes resting on rigid or deformable foundations

R.H. Plaut*, S.A. Cotton

The Charles E. Via, Jr. Department of Civil and Environmental Engineering, Virginia Polytechnic Institute and State University, Blacksburg, VA 24061-0105, USA

Received 17 July 2003; accepted 18 February 2004
Available online 17 September 2004

Abstract

Geomembrane tubes may be used as an alternative to sandbags for flood protection. The static and dynamic behavior of such tubes is considered, in the absence of external water. A two-dimensional analysis of a cross section of the tube is conducted. The tube is inflated with air, and the weight of the tube causes the equilibrium shape to be noncircular. The material is assumed to be inextensible and to have no bending resistance. Equilibrium configurations and small vibrations about equilibrium are investigated for tubes on rigid, Winkler, and Pasternak foundations. The mode shape corresponding to the lowest frequency is symmetric with two nodes. The effects of the internal pressure, foundation stiffness, and foundation shear modulus on the first four frequencies and modes are determined numerically using a shooting method.

1. Introduction

This research is part of a study on the use of inflated tubes as an alternative to sandbags for restraining floodwaters. Web sites of manufacturers of such unanchored tubes include Refs. [1–6]. Most of these tubes are inflated with water, but one of the manufacturers fills the tubes with air, and an attached apron (skirt) lies under the external floodwater; frictional resistance of the apron with the ground inhibits rolling or sliding of the tube [3].

*Corresponding author. Tel.: +1-5402316072; fax: +1-5402317532.
E-mail address: rplaut@vt.edu (R.H. Plaut).

0022-460X/$ - see front matter © 2004 Elsevier Ltd. All rights reserved.
doi:10.1016/j.jsv.2004.02.032

Related to these freestanding tubes are anchored inflatable dams. They are used for a variety of purposes, such as increasing the height of existing dams or spillways, impounding water for recreational basins, diverting water for irrigation or groundwater recharging, controlling water flow for hydroelectric production, and preventing river backflows caused by high tides. Publications involving the vibrations of these anchored tubes include Refs. [7–16].

With regard to unanchored tubes, equilibrium configurations for liquid-filled tubes have been investigated previously (e.g., Refs. [17,18] and other studies cited therein). Stacked tubes were treated in Ref. [19], with one tube on top of another tube or on top of a pair of tubes in a pyramid configuration. In Refs. [17,19], both rigid and deformable foundations were considered. Ref. [20] describes a numerical investigation of a water-filled tube resting on the ground and subjected to external water on one side, with a wedge placed on the other side to inhibit rolling or sliding. Vibrations of these tubes have not been analyzed previously.

The tube considered here is inflated with air, and the weight of the tube is included, so that the cross section is not circular. The bending stiffness of the tube is neglected (i.e., the tube is treated as a membrane), and the material is assumed to be inextensible. The tube is long, and a two-dimensional analysis is conducted. The equilibrium shape is determined first, and then small vibrations of the cross section about its equilibrium shape are analyzed. In Section 2, the problem is formulated for a tube resting on a rigid, horizontal foundation, and associated vibration frequencies and mode shapes are presented in Section 3. Deformable Winkler and Pasternak foundations are considered in Section 4, followed by numerical results in Section 5. Section 6 contains concluding remarks.

2. Formulation for rigid foundation

Fig. 1 shows the cross section of a tube resting on a rigid foundation. Friction between the tube and the foundation is neglected. The origin O for this case is at the right end of the contact region. The coordinates are $X(S,T)$ and $Y(S,T)$, and the angle of the tangent with the horizontal is $\theta(S,T)$, where S is the arc length and T is time. The total perimeter is L, the contact length is B, the internal air pressure is P, the mass per length of the tube is μ, the coefficient of viscous damping is C, and the tension in the tube is $Q(S,T)$. Damping will not be included in the analysis presented here, but will be included in one set of results.

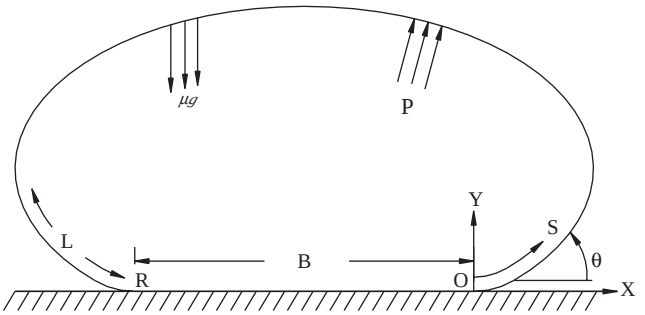

Fig. 1. Equilibrium configuration, forces, and coordinates for rigid foundation.

If the reaction force per unit length is denoted F, then overall equilibrium of vertical forces yields $FB = \mu gL$, and equilibrium of a free-body diagram of the tube along the foundation gives $FB = (P + \mu g)B$. Eliminating F provides the equation $B = \mu gL/(P + \mu g)$ for the contact length.

For the range $0 < S < L - B$, geometrical relationships are

$$\frac{\partial X}{\partial S} = \cos\,\theta, \quad \frac{\partial Y}{\partial S} = \sin\,\theta. \tag{1a, b}$$

Based on the free-body diagram in Fig. 2, with K, G_P, and C equal to zero, dynamic equilibrium of forces in the tangential and normal directions yields

$$\mu\frac{\partial^2 X}{\partial T^2}\cos\,\theta + \mu\frac{\partial^2 Y}{\partial T^2}\sin\,\theta = \frac{\partial Q}{\partial S} - \mu g\,\sin\,\theta, \tag{2a}$$

$$\mu\frac{\partial^2 Y}{\partial T^2}\cos\,\theta - \mu\frac{\partial^2 X}{\partial T^2}\sin\,\theta = Q\frac{\partial \theta}{\partial S} - P - \mu g\,\cos\,\theta. \tag{2b}$$

The analysis is carried out in terms of the nondimensional quantities

$$x = \frac{X}{L}, \quad y = \frac{Y}{L}, \quad s = \frac{S}{L}, \quad b = \frac{B}{L}, \quad q = \frac{Q}{\mu gL}, \quad p = \frac{P}{\mu g}, \quad t = T\sqrt{\frac{g}{L}},$$
$$\omega = \Omega\sqrt{\frac{L}{g}}, \quad h_f = \frac{H_f}{L}, \quad c = \frac{C}{\mu}\sqrt{\frac{L}{g}}, \quad k = \frac{KL}{\mu g}, \quad g_P = \frac{G_P}{\mu gL}, \tag{3}$$

where Ω is a vibration frequency.

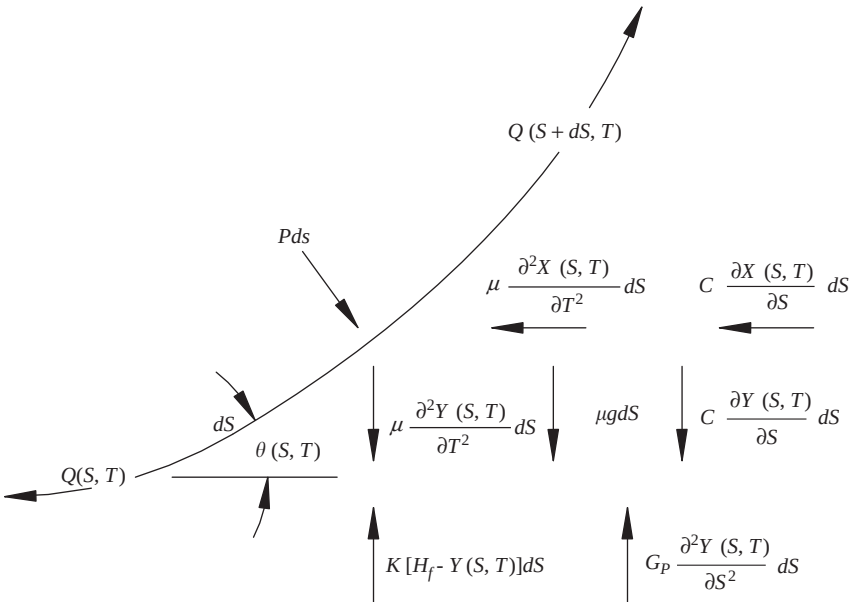

Fig. 2. Free-body diagram including inertia, damping, and deformable foundation forces.

The coordinates, rotation, and tension are written in the form

$$x(s,t) = x_e(s) + x_d(s)\sin\,\omega t, \quad y(s,t) = y_e(s) + y_d(s)\sin\,\omega t,$$
$$\theta(s,t) = \theta_e(s) + \theta_d(s)\sin\,\omega t, \quad q(s,t) = q_e(s) + q_d(s)\sin\,\omega t, \tag{4a–d}$$

where subscripts e and d represent equilibrium and dynamic quantities, respectively. Eqs. (4) are substituted into Eqs. (1) and (2), and the resulting equations are linearized in the dynamic quantities. The terms independent of time provide the following governing equations for equilibrium:

$$\frac{dx_e}{ds} = \cos\,\theta_e, \quad \frac{dy_e}{ds} = \sin\,\theta_e, \tag{5a, b}$$

$$\frac{d\theta_e}{ds} = \frac{p + \cos\,\theta_e}{q_e}, \quad \frac{dq_e}{ds} = \sin\,\theta_e. \tag{6a, b}$$

The remaining terms lead to the following equations governing small vibrations about equilibrium:

$$\frac{dx_d}{ds} = -\theta_d \sin\,\theta_e, \quad \frac{dy_d}{ds} = \theta_d \cos\,\theta_e, \tag{7a, b}$$

$$\frac{d\theta_d}{ds} = \frac{1}{q_e}\left[\omega^2(x_d \sin\,\theta_e - y_d \cos\,\theta_e) - \theta_d \sin\,\theta_e - q_d\frac{(p + \cos\,\theta_e)}{q_e}\right], \tag{8a}$$

$$\frac{dq_d}{ds} = -\omega^2(x_d \cos\theta_e + y_d \sin\theta_e) + \theta_d \cos\theta_e \tag{8b}$$

3. Results for rigid foundation

Equilibrium configurations are determined first. Based on Eqs. (5b) and (6b), one can write $q_e(s) = y_e(s) + q_0$ where q_0 is the tension at $s = 0$. This is used in Eq. (6a), and then Eqs. (5a,b) and (6a), as well as all other sets of equations to be treated, are solved using a shooting method and the computer program Mathematica [21]. The boundary conditions at $s = 0$ (point O) are $x_e = y_e = \theta_e = 0$. The nondimensional internal air pressure p is specified, and $b = 1/(p + 1)$ from the equilibrium arguments above. The tension parameter q_0 is varied until the boundary condition $\theta_e = 2\pi$ at $s = 1 - b$ (point R in Fig. 1) is satisfied with sufficient accuracy. (The conditions $x_e = -b$ and $y_e = 0$ at point R are satisfied automatically by the solution.) Alternatively, one could use symmetry and shoot to $s = (1b)/2$ where $x_e = -b/2$ and $\theta_e = \pi$.

Equilibrium shapes are presented in Fig. 3 for five values of nondimensional internal pressure p, which must be greater than unity for the pressure to overcome the weight of the tube. The nondimensional tube heights corresponding to $p = 1.05$, 2, 3, 4, and 5 are 0.050, 0.184, 0.225, 0.247, and 0.260, respectively. The associated values of the maximum tension, which occurs at the top of the tube, are $q = 0.0511$, 0.276, 0.450, 0.616, and 0.780.

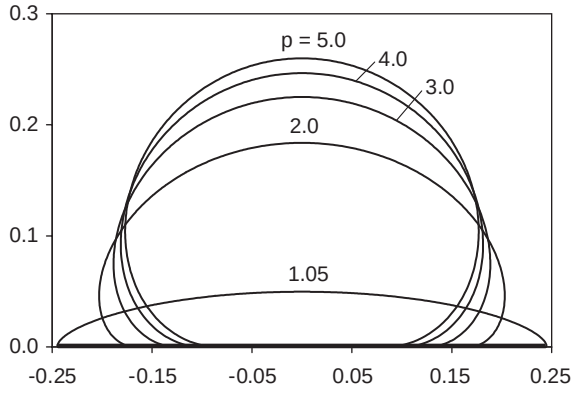

Fig. 3. Equilibrium configurations for tube on rigid foundation.

Now small vibrations about equilibrium are considered. The previous equilibrium solution for q_e is utilized. The equilibrium Eqs. (5) and (6) are augmented by the dynamic Eqs. (7) and (8). At $s = 0$, the boundary conditions are $y_d = \theta_d = 0$. In the shooting method, the initial condition $x_d(0)$ is specified as a modal amplitude, and the initial condition $q_d(0)$ and frequency ω are varied until the end conditions $y_d = \theta_d = 0$ are satisfied. For symmetric modes, the arc length at the end of the raised part of the tube is at $s = 1 - b - 2x_d(0)$, since the tube displaces outward the same amount at points O and R in Fig. 1; for anti-symmetric modes the end is at $s = 1 - b$, since the tube displaces horizontally by equal amounts in the same direction at O and R. The initial guess for the frequency is placed in different ranges so as to obtain the lowest four vibration frequencies and corresponding modes.

The first four mode shapes for $p = 3$ are shown in Fig. 4, along with the equilibrium shape. The corresponding frequencies are $\omega = 5.02$, 8.37, 11.4, and 14.3. The first mode is symmetric with two nodes, the second is anti-symmetric with three nodes, and so on. The same forms occur for other cases. A mode with no nodes does not occur, since the tube is inextensible and the curvature of the equilibrium shape does not change sign. Also, a mode with one node does not exist. For anchored tubes with two supports (e.g., at O and R in Fig. 1), the first mode is anti-symmetric with a single node [7]. Here, however, the tube would roll to one side if put in such a shape, rather than vibrating about the equilibrium configuration.

For nondimensional pressure p in the range $1.05 < p < 5$, the variations of the first four frequencies with p are plotted in Fig. 5. The rate of increase of ω with p decreases as p increases.

Next, viscous damping is considered. The damping forces involving the coefficient C in Fig. 2 are included. The quantity ω^2 in Eqs. (8) is replaced by $\omega^2 - ic\omega$. The real part of the resulting complex quantity ω gives the oscillating frequency of the decaying free motion (i.e., the damped frequency), and is plotted in Fig. 6 as a function of the nondimensional damping coefficient c for the case $p = 3$. The damped frequency decreases as the damping coefficient increases. When one of the frequencies reduces to zero, the corresponding modal motion becomes overdamped. Results for other values of p are given in Ref. [22].

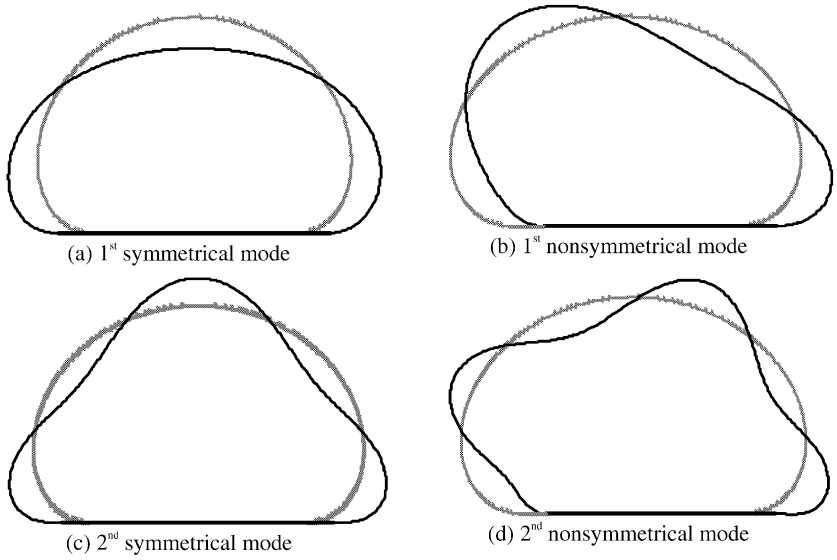

Fig. 4. First four vibration modes when $p = 3$: (a) first mode (symmetric); (b) second mode (anti-symmetric); (c) third mode (symmetric); (d) fourth mode (anti-symmetric).

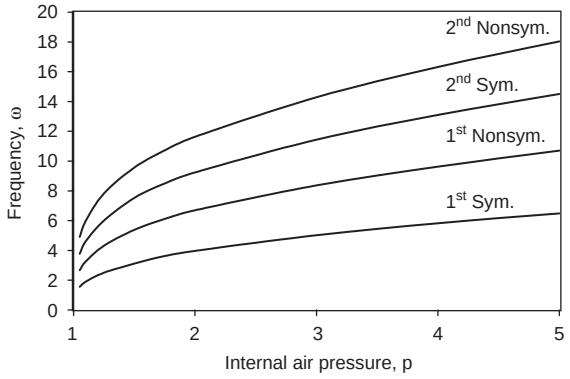

Fig. 5. First four vibration frequencies versus internal pressure.

4. Formulation for deformable foundation

It is assumed now that the tube rests on a Pasternak foundation, with a Winkler foundation included as a special case. The cross section is depicted in Fig. 7, where K is the elastic Winkler coefficient (representing a continuum of linear vertical springs) and G_P is the shear stiffness for a Pasternak layer [23]. Now the origin of the coordinate system is at the bottom of the tube, which has settlement H_f below the foundation level. When the tube displaces downward into the foundation, the upward forces are proportional to this displacement and to its second derivative (which approximates the curvature), as shown in Fig. 2.

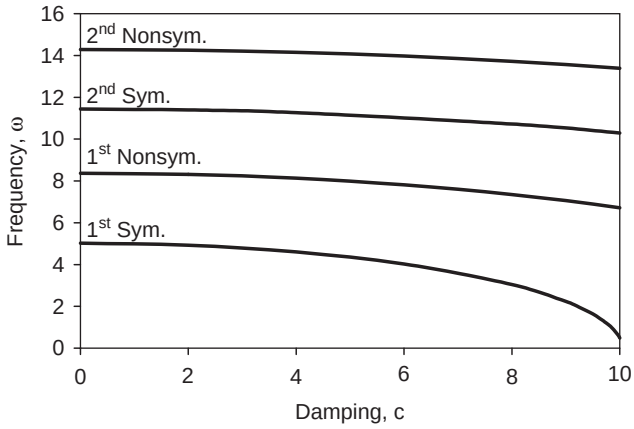

Fig. 6. First four damped frequencies versus damping coefficient when $p = 3$.

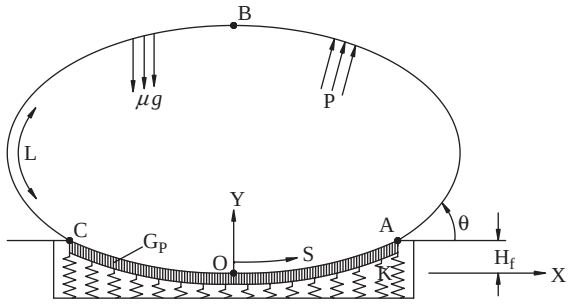

Fig. 7. Equilibrium configuration, forces, and coordinates for deformable foundation.

The nondimensional quantities in Eq. (3) are used in the analysis. For no damping, the governing equations are the two geometrical relationships as before and, for $y<h_f$,

$$q\frac{\partial\theta}{\partial s}=\frac{\partial^2 y}{\partial t^2}\cos\theta-\frac{\partial^2 x}{\partial t^2}\sin\theta+p+\cos\theta-k(h_f-y)\cos\theta-g_P\frac{\partial^2 y}{\partial s^2}\cos\theta, \tag{9a}$$

$$\frac{\partial q}{\partial s}=\frac{\partial^2 x}{\partial t^2}\cos\theta+\frac{\partial^2 y}{\partial t^2}\sin\theta+\sin\theta-k(h_f-y)\sin\theta-g_P\frac{\partial^2 y}{\partial s^2}\sin\theta. \tag{9b}$$

For $y>h_f$, the terms involving k and g_P are deleted from Eqs. (9) and subsequent equations.

For equilibrium, Eqs. (5) are valid, along with

$$\frac{\mathrm{d}\theta_e}{\mathrm{d}s}=\frac{1}{q_e}\left[k(y_e-h_f)\cos\theta_e-g_P\frac{\mathrm{d}^2 y_e}{\mathrm{d}s^2}\cos\theta_e+p+\cos\theta_e\right], \tag{10a}$$

$$\frac{\mathrm{d}q_e}{\mathrm{d}s}=\left[k(y_e-h_f)-g_P\frac{\mathrm{d}^2 y_e}{\mathrm{d}s^2}+1\right]\sin\theta_e, \tag{10b}$$

when $y<h_f$. Differentiation of Eq. (5b) yields

$$\frac{d^2y_e}{ds^2}=\frac{d\theta_e}{ds}\cos\theta_e \tag{11}$$

which is used in Eqs. (10). Then Eq. (10a) is written in the form

$$\frac{d\theta_e}{ds}=\frac{k(y_e-h_f)\cos\theta_e+p+\cos\theta_e}{q_e+g_P\cos^2\theta_e}, \tag{12}$$

and Eqs. (5a), (5b), (10b), and (12) form a system of first-order equations for $x_e(s)$, $y_e(s)$, $q_e(s)$, and $\theta_e(s)$. An "If" statement is used in Mathematica to handle the changes in the equations when y becomes larger than h_f (i.e., at point A in Fig. 7).

For small vibrations about equilibrium, Eqs. (4) are used in Eqs. (9) and the procedure used in Section 2 is applied. Eqs. (7) are again applicable, along with

$$\begin{aligned}q_d\frac{d\theta_e}{ds}+q_e\frac{d\theta_d}{ds}&=\omega^2\left(x_d\sin\theta_e-y_d\cos\theta_e\right)-\theta_d\sin\theta_e\\&\quad+k(h_f-y_e)\theta_d\sin\theta_e+ky_d\cos\theta_e+g_P\frac{d^2y_e}{ds^2}\theta_d\sin\theta_e-g_P\frac{d^2y_d}{ds^2}\cos\theta_e,\end{aligned} \tag{13a}$$

$$\begin{aligned}\frac{dq_d}{ds}&=-\omega^2\left(x_d\cos\theta_e+y_d\sin\theta_e\right)+\theta_d\cos\theta_e-k(h_f-y_e)\theta_d\cos\theta_e\\&\quad+ky_d\sin\theta_e-g_P\frac{d^2y_e}{ds^2}\theta_d\cos\theta_e-g_P\frac{d^2y_d}{ds^2}\sin\theta_e.\end{aligned} \tag{13b}$$

By differentiating Eq. (7b), one obtains

$$\frac{d^2y_d}{ds^2}=\frac{d\theta_d}{ds}\cos\theta_e-\frac{d\theta_e}{ds}\theta_d\sin\theta_e. \tag{14}$$

With the use of Eqs. (11), (12), and (14), Eqs. (13) can be written as first-order equations in θ_d and q_d.

5. Results for deformable foundation

To obtain equilibrium configurations, the parameters p, k, and g_P are specified, and Eqs. (5) and (10) are solved. At $s=0$ (the bottom of the tube), $x_e=y_e=\theta_e=0$. The initial condition $q_e(0)$ and the maximum settlement h_f are varied until the conditions $x_e=0$ and $\theta_e=\pi$ are satisfied at $s=0.5$ (the top of the tube, i.e., point B in Fig. 7).

For the Winkler foundation, i.e., with $g_P=0$, equilibrium shapes are plotted in Fig. 8 for $p=2$ and $k=100$, 200, and ∞ (i.e., a rigid foundation). Pasternak foundations are considered in Fig. 9, with $p=2$, $k=200$, and $g_P=0$ (Winkler foundation), 1.5, and 30. As either k or g_P increases, the settlement decreases.

Vibration frequencies and modes are computed with the use of Eqs. (7) and (13) in first-order form, together with the equilibrium Eqs. (5) and (10) and their solutions for $q_e(0)$ and h_f. For symmetric modes, at $s=0$ the values of x_d and θ_d are 0, y_d is specified, and q_d is an unknown

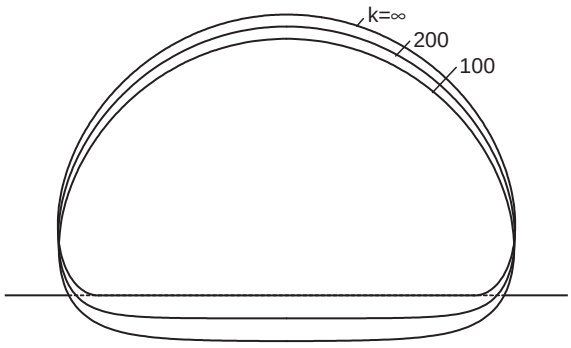

Fig. 8. Equilibrium configurations for tube on Winkler foundation when $p = 2$.

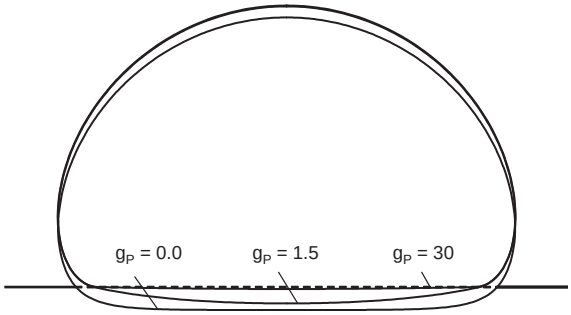

Fig. 9. Equilibrium configurations for tube on Pasternak foundation when $p = 2$ and $k = 200$.

(along with the frequency ω), and the shooting conditions at $s = 0.5$ are $x_d = \theta_d = 0$. For anti-symmetric modes, the only changes are that $\theta_d(0)$ is specified and $y_d(0)$ is zero.

The first four vibration modes are shown in Fig. 10, along with the equilibrium configuration, for the case $p = 2$, $k = 200$, and $g_P = 0$. The effect of the Winkler coefficient k on the first four vibration frequencies is shown in Fig. 11 for the case $p = 2$ and $g_P = 0$. The lowest two frequencies are barely affected in the range $40 < k < 200$ shown, while the next two frequencies increase and then level off. Fig. 12 illustrates how the shear modulus of the foundation affects the first four frequencies for the case $p = 2$ and $k = 200$. The frequencies decrease as g_P increases from zero, with an initial high rate of reduction. This unexpected behavior is related to the change in the equilibrium shape as g_P is increased.

Another type of deformable foundation involves the Winkler springs plus a stretched membrane below the structure. It is called a Filonenko–Borodich foundation [22]. For small slopes of the tube, it can be approximated by the forces in the Pasternak model with g_P replaced by the nondimensional constant tension t_{FB} in the supporting membrane. If the slope is not always small for $y < h_f$, then the Pasternak forces are replaced by a tangential force. The quantity q_e in Eqs. (6), (10), (12), and (13) is replaced by $q_e + t_{FB}$, the quantity q in Eqs. (9) is replaced by $q + t_{FB}$, and g_P is set equal to zero. For the examples involving a Pasternak foundation here, if the

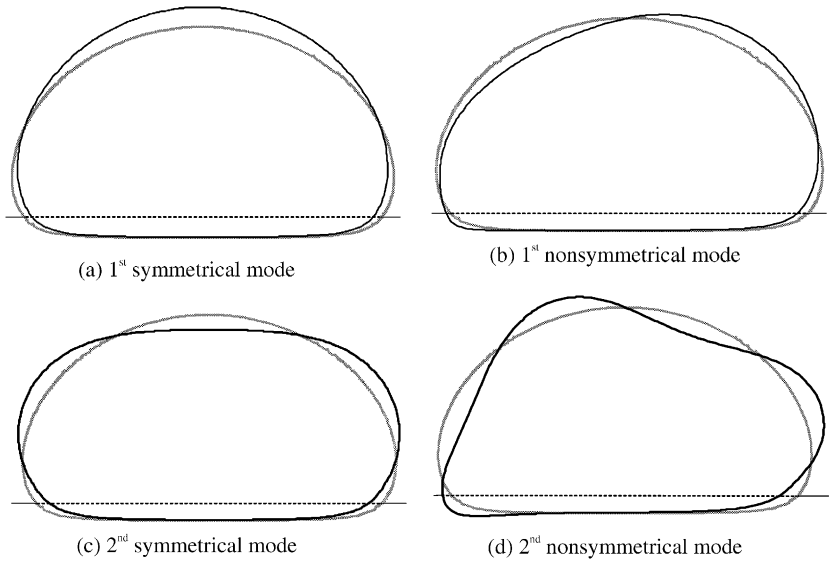

Fig. 10. First four vibration modes when $p = 2$ and $k = 200$: (a) first mode (symmetric); (b) second mode (anti-symmetric); (c) third mode (symmetric); (d) fourth mode (anti-symmetric).

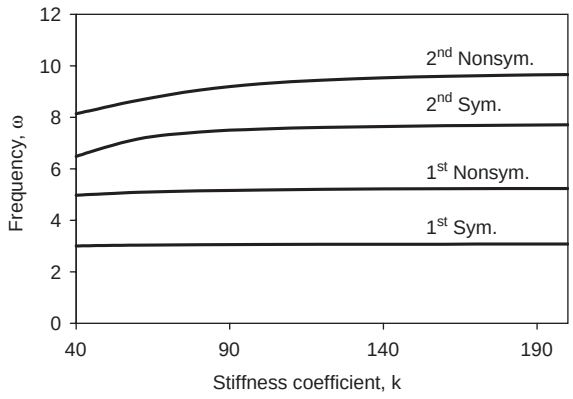

Fig. 11. First four frequencies versus Winkler coefficient when $p = 2$ and $g_P = 0$.

Pasternak shear layer is replaced by a Filonenko–Borodich membrane with $g_P = t_{FB}$, the numerical vibration results are almost the same.

6. Concluding remarks

Long air-filled tubes resting on a rigid or deformable foundation have been considered. The self-weight of the tube was included in the analysis. The material was assumed to behave like an

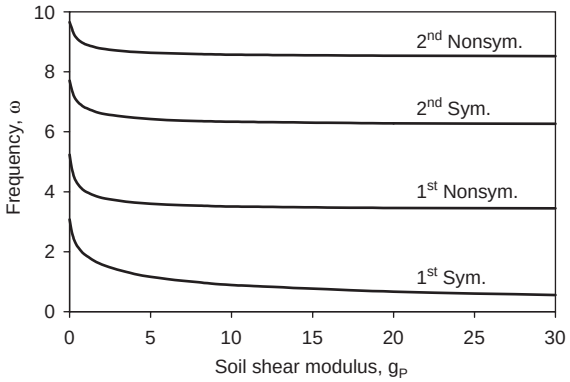

Fig. 12. First four frequencies versus foundation shear modulus when $p = 2$ and $k = 200$.

inextensible membrane, so that it had no bending stiffness. A rigid foundation was treated first. The governing equations for equilibrium and for small vibrations about equilibrium were formulated and solved numerically. The first four frequencies and modes were determined numerically for a given internal pressure. As the internal air pressure increases, the frequencies increase. An increase of damping lowers the damped vibration frequency, and modes can become overdamped.

A similar analysis was carried out for a Winkler foundation and for a Pasternak foundation. The frequencies increase with an increase in the spring stiffness (i.e., the Winkler coefficient), but decrease with an increase in the shear modulus of the foundation.

The shooting method was effective in computing the unknown parameters in the governing equilibrium and vibration equations. Unlike the case of anchored inextensible tubes, these tubes do not exhibit a mode with a single node. Therefore, the lowest frequency here is associated with a symmetric mode having two nodes. The vibration modes alternate being symmetric or anti-symmetric, and the nth mode has $n + 1$ nodes.

Acknowledgement

This research was supported by the US National Science Foundation under Grant No. CMS-9807335.

References

[1] http://www.aquabarrier.com.
[2] http://www.geocheminc.com/wstructures.htm.
[3] http://www.noaq.com.
[4] http://www.superiordam.com.
[5] http://www.usfloodcontrol.com.

[6] http://www.waterstructures.com.
[7] R.H. Plaut, T.D. Fagan, Vibrations of an inextensible, air-inflated, cylindrical membrane, *Journal of Applied Mechanics* 55 (1988) 672–675.
[8] R.H. Plaut, M.J. Leeuwrik, Nonlinear oscillations of an inextensible, air-inflated, cylindrical membrane, *International Journal of Non-Linear Mechanics* 23 (1988) 347–353.
[9] J.-C. Hsieh, R.H. Plaut, O. Yucel, Vibrations of an inextensible cylindrical membrane inflated with liquid, *Journal of Fluids and Structures* 3 (1989) 151–163.
[10] R.H. Plaut, Parametric excitation of an inextensible, air-inflated, cylindrical membrane, *International Journal of Non-Linear Mechanics* 25 (1990) 253–262.
[11] J.-C. Hsieh, R.H. Plaut, Free vibrations of inflatable dams, *Acta Mechanica* 85 (1990) 207–220.
[12] J. Wauer, R.H. Plaut, Vibrations of an extensible, air-inflated, cylindrical membrane, *Zeitschrift für angewandte Mathematik und Mechanik* 71 (1991) 191–192.
[13] C.M. Dakshina Moorthy, J.N. Reddy, R.H. Plaut, Three-dimensional vibrations of inflatable dams, *Thin-Walled Structures* 21 (1995) 291–306.
[14] P.-H. Wu, R.H. Plaut, Analysis of the vibrations of inflatable dams under overflow conditions, *Thin-Walled Structures* 26 (1996) 241–259.
[15] R.H. Plaut, S.I. Liapis, D.P. Telionis, When the levee inflates, *Civil Engineering (ASCE)* 68 (1) (1998) 62–64.
[16] G.V. Mysore, S.I. Liapis, R.H. Plaut, Dynamic analysis of single-anchor inflatable dams, *Journal of Sound and Vibration* 215 (1998) 251–272.
[17] R.H. Plaut, S. Suherman, Two-dimensional analysis of geosynthetic tubes, *Acta Mechanica* 129 (1998) 207–218.
[18] S. Cantré, Geotextile tubes—analytical design aspects, *Geotextiles and Geomembranes* 20 (2002) 305–319.
[19] R.H. Plaut, C.R. Klusman, Two-dimensional analysis of stacked geosynthetic tubes on deformable foundations, *Thin-Walled Structures* 34 (1999) 179–194.
[20] T.C. Huong, R.H. Plaut, G.M. Filz, Wedged geomembrane tubes as temporary flood-fighting devices, *Thin-Walled Structures* 40 (2001) 913–923.
[21] S. Wolfram, *The Mathematica Book*, third ed., Cambridge University Press, Cambridge, UK, 1996.
[22] S.A. Cotton, Two-Dimensional Vibrations of Inflated Geosynthetic Tubes Resting on a Rigid or Deformable Foundation, MS Thesis, Virginia Polytechnic Institute and State University, Blacksburg, VA, 2003.
[23] A.P.S. Selvadurai, *Elastic Analysis of Soil–Foundation Interaction*, Elsevier, New York, 1979.